Corticospinal excitability is facilitated during coordinative action observation and motor imagery of adapted single-leg sit-to-stand movements in young healthy adults

Ashika Chembila Valappil[1], Neža Grilc[2], Federico Castelli[1], Samantha Chye[1], David J. Wright[3], Christopher J. Tyler[1], Ryan Knight[1], Omar S. Mian[1], Neale A. Tillin[1], Adam M. Bruton[1,2]

Author Note: Ashika Chembila Valappil is the first author for this manuscript. *Adam Bruton is the corresponding author for this manuscript: adam.bruton@brunel.ac.uk, HNZW 271, Heinz Wolff Building, Brunel University of London, Uxbridge, UB8 3PH, United Kingdom

[1] School of Life and Health Sciences, University of Roehampton, United Kingdom
[2] Department of Sport, Health and Exercise Sciences, Brunel University of London, United Kingdom
[3] School of Psychology, Manchester Metropolitan University, United Kingdom

Abstract

Combined action observation and motor imagery (AOMI) facilitates corticospinal excitability (CSE). This study used single-pulse transcranial magnetic stimulation (TMS) to explore changes in CSE for *coordinative* AOMI of a single-leg sit-to-stand (SL-STS) movement. Twenty-one healthy adults completed two testing sessions, where they engaged with baseline (BL), action observation (AO), and motor imagery (MI) control conditions, and three experimental conditions where they observed a *slow-paced* SL-STS while simultaneously imagining a *slow-* ($AOMI_{HICO}$), *medium-* ($AOMI_{MOCO}$), or *fast-paced* ($AOMI_{LOCO}$) SL-STS. A TMS pulse was delivered to the right leg representation of the left primary motor cortex at three stimulation timepoints aligned with peak EMG activity of the knee extensor muscle group for the *slow-paced* (T3), *medium-paced* (T2), and *fast-paced* (T1) SL-STS during each condition. Motor evoked potential (MEP) amplitudes were recorded from the knee extensor muscle group as a marker of CSE for all stimulation timepoints and conditions. A main effect for experimental condition was reported for all stimulation timepoints. MEP amplitudes were significantly greater for $AOMI_{HICO}$ at T1 and T3, and $AOMI_{MOCO}$ and $AOMI_{LOCO}$ at all stimulation timepoints, when compared with control conditions. This study provides neurophysiological evidence supporting the use of *coordinative* AOMI as an alternative method for movement (re)learning.

Keywords: Transcranial Magnetic Stimulation, Motor Evoked Potential, Dual-Action Simulation, Visual Guidance Hypothesis, Mental Simulation

Introduction

Action observation (AO) is the process of purposefully observing human movement via video or live demonstration (Eaves et al., 2022), while motor imagery (MI) involves the internal mental rehearsal of one's own movement execution (MacIntyre et al., 2013). Both AO and MI are effective interventions for enhancing movement execution and (re)learning in rehabilitation and care settings (e.g., Buccino, 2014; Herranz-Gómez et al., 2020; Nicholson et al., 2019). These improvements have been explained by motor simulation theory, which posits that AO and MI activate brain areas associated with movement planning, production, and control, and thus have the capacity to increase functional connectivity across these motor networks (Jeannerod, 2001). In support of this proposition, research employing a range of neuroscientific modalities (i.e., fMRI, fNIRS, EEG, TMS) demonstrates increased cortico-motor activity for both AO and MI compared to control/baseline conditions (see e.g., Condy et al., 2021; Grosprêtre et al., 2015; Hardwick et al., 2018). Literature to-date has typically compared these two forms of motor simulation, showing that brain activation patterns for AO and MI are distinct, but overlapping (Hardwick et al., 2018), and that both AO and MI facilitate corticospinal excitability (CSE) as a marker of corticomotor activity compared to control conditions (e.g., Clark et al., 2004; Williams et al., 2012). After an initial review by Vogt et al. (2013), a body of work has investigated the behavioral outcomes and underlying neurophysiological mechanisms associated with the combined and simultaneous use of AO and MI.

Combined action observation and motor imagery (AOMI) involves a person observing human movement and simultaneously imagining the physiological sensations and kinesthetic experiences associated with executing the same or a different movement (Eaves, Riach, et al., 2016, Eaves et al., 2022). A recent meta-analysis by Chye et al. (2022) synthesized literature on highly-coordinated AOMI (AOMIHICO), where a person watches a movement demonstration and imagines the feeling of executing an identical movement in the same perspective in time with the viewed content. This meta analysis

reported improved movement outcomes and facilitation of CSE for AOMI compared to AO and control conditions, but not compared to MI conditions. The behavioral and neurophysiological findings from Chye et al.'s (2022) meta-analysis suggest that $AOMI_{HICO}$ benefits motor execution due to strong and widespread activation of movement-related brain regions. Specifically, repeated engagement in $AOMI_{HICO}$ is likely to induce plastic-like changes in the motor system, benefitting physical execution of the movement in a similar manner to physical training (Chye et al., 2022; Grilc et al., 2024). This sentiment is supported in a rehabilitation context, as studies employing TMS show that $AOMI_{HICO}$ leads to increased facilitation of CSE for whole-body functional movements such as walking (e.g., Kaneko et al., 2018) and balance (e.g., Mouthon et al., 2015, 2016), and studies employing $AOMI_{HICO}$ as a training intervention report improved muscle strength (Scott et al., 2018), rehabilitation outcomes (Marusic et al., 2018), and postural control (Taube et al., 2014) across the lifespan.

Whilst empirical support for $AOMI_{HICO}$ is growing, there is limited research on alternative forms of AOMI. Vogt et al. (2013) proposed that AOMI can occur along a spectrum, whereby AO and MI serve different roles during AOMI depending on the level of coordination between the two. At one end of this spectrum is *congruent* AOMI, where the content and/or visual perspective are identical for AO and MI components of AOMI. The term $AOMI_{HICO}$ has been adopted instead of *congruent* AOMI in this study, as it has been proposed that the AO and MI components are never fully *congruent* during AOMI (Frank et al., 2020). This proposition was largely based on the different modalities adopted for AO (visual and auditory) and MI (kinesthetic) components in Vogt et al.'s (2013) definition for *congruent* AOMI, however it is worth noting that parameters such as body structure, movement pattern, and imagery ability will also result in an offset between AO and MI during AOMI of the same action, making $AOMI_{HICO}$ a more suitable term. On the other end of the spectrum lies *conflicting* AOMI, where the content and/or visual perspective for AO and MI components of AOMI are opposing (e.g., watching movement and imagining being still and relaxed). In between these endpoints lies *coordinative* AOMI, where the

content and/or visual perspective for AO and MI components of AOMI is similar. For this type of AOMI, the level of coordination between the observed or imagined actions can vary on a range of movement parameters, including the type, direction, speed, force, and accuracy of the movement (Chye et al., 2022; Grilc et al., 2024).

Two main theoretical hypotheses have been proposed to explain the underlying mechanisms for *coordinative* AOMI. The first is the Dual-Action Simulation Hypothesis (DASH) account for AOMI proposed by Eaves, Riach et al. (2016). Drawing from the Affordance-Competition Hypothesis (Cisek, 2007), the DASH suggests that individuals generate separate motor representations for the observed and imagined actions during AOMI, and that these are maintained as parallel sensorimotor streams that either merge or compete depending on the level of coordination between the observed and imagined actions. For $AOMI_{HICO}$ these likely merge as one sensorimotor stream, producing more widespread activation in the premotor cortex compared to AO or MI alone. For lowly-coordinated AOMI ($AOMI_{LOCO}$), where there is little overlap between the AO and MI components, the DASH proposes that visuo-motor representations for the observed and imagined actions are likely to compete as separate sensorimotor streams. This would result in similar cortico-motor activity to performing the AO or MI tasks in isolation, depending on which simulation process is prioritized based on relevance to the ongoing motor plan. For moderately-coordinated AOMI ($AOMI_{MOCO}$), the visuo-motor representations of the observed and imagined movements may either merge or compete. This is dependent on the amount of transferable sensorimotor information between the two simulated movements and the relevance of these to the ongoing movement plan. Based on this proposition, $AOMI_{MOCO}$ can result in more widespread pre-motor activity via merged sensorimotor streams, or similar activity to AO or MI alone through prioritization of one competing sensorimotor stream, depending on the level of coordination between the two simulated movements during this type of AOMI.

The Visual Guidance Hypothesis (VGH; Meers et al., 2020) has been proposed as an alternative account for the processes involved in *coordinative* AOMI. The VGH argues that the imagined action is prioritized, with the observed action serving as an external visual stimulus that may facilitate or disrupt the imagined action during *coordinative* AOMI. According to the VGH, the increased cortico-motor activity reported in previous literature for $AOMI_{HICO}$ (see Chye et al., 2022 for a recent meta-analysis) is due to the observed action displaying *the same movement* and acting as a visual primer that forms a stronger motor representation for the imagined action. For $AOMI_{LOCO}$, the VGH suggests that a motor representation will only be formed for the imagined action due to the observed action displaying *another movement* and acting as a visual distractor. Unless ignored, this will disrupt the generation and maintenance of the imagined action, meaning cortico-motor activity will be reduced compared to independent MI. In a similar vein to $AOMI_{LOCO}$, the VGH proposes that a motor representation will only be formed for the imagined action during $AOMI_{MOCO}$ due to the observed action displaying *another movement*. However, the observed action might act as a visual primer or visual distractor during $AOMI_{MOCO}$ depending on the amount of transferable sensorimotor information between the two simulated movements. It is therefore possible that the observed action can both facilitate and disrupt the generation and maintenance of the imagined action, leading to either increased, similar, or decreased cortico-motor activity compared to independent MI.

Single-pulse transcranial magnetic stimulation (TMS) is the most prevalent neuroscientific modality adopted in the AOMI literature as it has high temporal resolution and can be used to determine the specific contributions for observed and imagined actions during AOMI (Chye et al., 2022). However, only three studies have used TMS to examine the neurophysiological markers for *coordinative* AOMI, and reported somewhat conflicting findings (Bruton et al., 2020; Meers et al., 2020; Grilc et al., 2024). Bruton et al. (2020) used a *coordinative* AOMI task where participants observed an index finger abduction-adduction movement while imagining the same movement with their little finger. They found

that CSE was facilitated in the muscles controlling both the observed and imagined movements, when controlling for visual attention on the observed movement, supporting the DASH. Conversely, using a similar finger movement task, Meers et al. (2020) found that CSE was only facilitated for the muscles involved in the imagined finger movement, with no such facilitation for the observed finger movement during *coordinative* AOMI, in line with the VGH. In a recent TMS study, Grilc et al. (2024) utilized two different *coordinative* AOMI tasks where coordination between the observed and imagined actions was based on different movement parameters. Both *coordinative* AOMI tasks involved observation of a knee extension movement, with one task involving imagined plantarflexion of the foot, a movement that is typically coupled with a knee extension movement when the body is propelled forward or upward by the legs (i.e., coordinated based on functional coupling), and one task involving imagined dorsiflexion of the foot, an action that rotates the foot in the same direction in the sagittal plane as the rotation to the shank produced by knee extension (i.e., coordinated based on movement direction). CSE was facilitated in the muscle controlling the imagined foot movement for both *coordinative* AOMI conditions, regardless of movement parameter, but no such facilitation was identified for muscles controlling the observed knee extension, aligning with the finding of Meers et al. (2020) and the VGH. Given the contrasting support for the predictions of the DASH (Bruton et al., 2020) and VHG (Meers et al., 2020; Grilc et al., 2024), both hypotheses warrant further empirical investigation by examining the neurophysiological markers of *coordinative* AOMI.

The limited research on *coordinative* AOMI may be due, in part, to the challenge of clearly defining the parameters that govern coordination between the two simulated actions. Both Bruton et al. (2020) and Meers et al. (2020) coordinated the observed and imagined actions based on movement type (finger abduction-adduction), whereas Grilc et al. (2024) employed two AOMI conditions that coordinated the observed and imagined actions based on different movement parameters (i.e., functional coupling vs movement direction). It is important to draw from literature on AO or MI when

140 considering possible movement parameters that might influence the ability to coordinate observed and
141 imagined actions, and the subsequent neurophysiological markers for *coordinative* AOMI. Several
142 studies have explored neurophysiological markers for AO and MI tasks with different force
143 requirements, showing that CSE is increased as a function of force production during both observed
144 (e.g., Alaerts et al., 2010, 2012; Helm et al., 2015) and imagined actions (e.g., Helm et al., 2015;
145 Mizuguchi et al., 2013). There are mixed findings regarding movement speed during AO, with studies
146 reporting decreased CSE (Moriuchi et al., 2014, 2017), no change in CSE (Moriuchi et al., 2017), and
147 increased CSE (Kitamura et al., 2023) as movement speed is increased for various upper-limb
148 movements. Given the close relationship between movement force and speed for dynamic actions,
149 where greater force often results in greater acceleration and thus velocity, manipulating one of these
150 parameters is of potential interest during *coordinative* AOMI.

151 This study aimed to test the DASH (Eaves, Riach, et al., 2016) and VGH (Meers et al., 2020)
152 propositions for *coordinative* AOMI by comparing CSE responses during AOMI conditions where
153 coordination between the observed and imagined actions varied based on movement speed. In this
154 experiment, all *coordinative* AOMI conditions involved observation of a *slow-paced* single-leg sit-to-
155 stand (SL-STS) movement but varied in the speed of the simultaneously imagined SL-STS. Specifically,
156 $AOMI_{HICO}$ involved simultaneous imagery of a *slow-paced* SL-STS, $AOMI_{MOCO}$ involved simultaneous
157 imagery of a *medium-paced* SL-STS, and $AOMI_{LOCO}$ involved simultaneous imagery of a *fast-paced* SL-STS
158 during observation of a *slow-paced* SL-STS, with audio sonification used to guide the imagery speed (see
159 Castro, Osman et al., 2021; Castro, Bryjka et al., 2021).

160 If the propositions of the DASH (Eaves, Riach, et al., 2016) are accurate, it is hypothesized that:
161 H1; CSE facilitation will be increased for the $AOMI_{HICO}$ condition at T3 (i.e., the stimulation timepoint
162 corresponding to peak EMG activity for the *slow-paced* SL-STS) due to the merging of sensorimotor
163 streams for AO and MI of the same action and movement speed. H2; CSE facilitation will be increased

for the $AOMI_{MOCO}$ condition at both T3 and T2 (i.e., the stimulation timepoint corresponding to peak EMG activity for the *medium-paced* SL-STS) due to the maintenance of sensorimotor streams for AO and MI of the same action with similar movement speeds. H3; CSE facilitation will not be increased for the $AOMI_{LOCO}$ condition at any stimulation timepoint due to the competition between sensorimotor streams for AO and MI of the same action with different movement speeds.

If the propositions of the VGH (Meers et al., 2020) are accurate, it is hypothesized that: H1; CSE facilitation will be increased for the $AOMI_{HICO}$ condition at T3 because the observed action will enhance the motor representation formed for the imagined action when the same movement type and speed are employed for both AO and MI simultaneously. H2; CSE facilitation will be increased for the $AOMI_{MOCO}$ condition at T2 due to prioritization of the imagined action during simultaneous AO and MI of the same action with similar movement speeds. H3; CSE facilitation will be increased for the $AOMI_{LOCO}$ condition at T1 due to prioritization of the imagined action during simultaneous AO and MI of the same action with different movement speeds.

Methods

Participants

Based on previous AOMI studies employing TMS (e.g., Bruton et al., 2020; Grilc et al., 2024; Wright et al., 2018), twenty-one healthy adults aged 21-43 years (14 male, M_{age} = 29.29 ± 6.78 years) with normal or corrected-to-normal vision took part in this study. All participants underwent screening and provided written informed consent prior to data collection. The screening included completion of the TMS Adult Safety Screen (TASS; Keel et al., 2001) and the Movement Imagery Questionnaire - 3 (MIQ-3; Williams et al., 2012). All participants were safe to take part in the study based on responses to the TASS. MIQ-3 scores indicated that the final study sample could easily generate internal visual (6.14 ± 0.66), external visual (5.71 ± 1.27), and kinesthetic (5.57 ± 1.22) imagery, confirming their ability to complete the experimental tasks.

188 **Experimental Design**

189 This study was conducted in accordance with the ethical guidelines and approval of the ethical
190 committee at the host university (ethical approval number LSC 21-346). All study procedures are
191 reported using parts A, B and C of the Guidelines for Reporting Action Simulation Studies checklist
192 (Moreno-Verdú et al., 2024) and experimental code and materials can be accessed via the Open Science
193 Framework: https://osf.io/5vjwe/. A repeated measures design was employed where participants
194 completed six conditions, split into three control conditions and three experimental conditions, with all
195 conditions repeated across two testing sessions. The three control conditions were: (i) a baseline (BL)
196 condition where participants looked at a fixation cross placed on a static image depicting the SL-STS
197 from the video stimuli (50% of trials) or a blank background (50% of trials), (ii) an action observation
198 (AO) condition where participants were required to observe a video of a model performing a *slow-paced*
199 SL-STS movement, and (iii) a motor imagery (MI) condition where participants were required to imagine
200 the feelings and sensations associated with performing a *slow-paced* SL-STS movement. The three
201 experimental conditions were: (iv) a highly-coordinated AOMI ($AOMI_{HICO}$) condition where participants
202 were asked to simultaneously observe a *slow-paced* SL-STS movement while imagining the feelings and
203 sensations of performing the same *slow-paced* SL-STS movement, (v) a moderately-coordinated AOMI
204 ($AOMI_{MOCO}$) condition where participants were asked to simultaneously observe a *slow-paced* SL- STS
205 movement while imagining the feelings and sensations of performing a *medium-paced* SL-STS
206 movement, and (vi) a lowly-coordinated AOMI ($AOMI_{LOCO}$) condition where participants were asked to
207 simultaneously observe a *slow-paced* SL-STS movement while imagining the feelings and sensations of
208 performing a *fast-paced* SL-STS movement.

209 The six conditions were presented in a semi-randomized order across participants (see Figure 1
210 for a visual depiction of the experimental design), consistent with previous TMS studies investigating
211 different forms of AOMI (e.g., Bruton et al., 2020; Grilc et al., 2024). The BL condition was delivered

212 across five blocks of six trials (i.e., blocks 1, 3, 5, 7, 9) to account for a possible ordering effect across the
213 experiment by recording comparator MEP amplitude data before each condition containing movement
214 simulation tasks. The AO condition was presented as block 2, before any MI instructions were provided,
215 to reduce the likelihood of participants engaging in spontaneous or deliberate MI during this condition
216 (see Bruton et al., 2020). The MI condition was presented as block 4, after AO, as it was deemed
217 necessary to have first exposed participants to visual stimuli of a SL-STS to facilitate their MI of the
218 action due to their naivety with this movement. The three experimental conditions involving
219 *coordinative* AOMI tasks were presented last (i.e., blocks 6, 8, and 10), with the order of these
220 counterbalanced across the study sample to avoid the possibility of an ordering effect for these
221 conditions.

222 **Target Movement**

223 Rising from a chair, often referred to as sit-to-stand (STS), is a task that requires strength,
224 balance, and coordination. In elderly individuals, especially those with functional limitations, STS
225 performance is associated with various measures of physiological function (Lord et al., 2002; Schenkman
226 et al., 1996) and the demands of this movement can approach or exceed strength capacity (Hughes et
227 al., 1996). This poses a high risk of falls (Robinovitch et al 2013), making it a task of significant
228 importance, especially in the maintenance of independent living for older adult populations (Slaughter
229 et al., 2015). Although a normal STS is a relatively unchallenging task for young individuals, it becomes
230 challenging in a manner that resembles the differences between young and older adults performing a
231 normal STS if performed on a single leg (SL-STS). For example, young adults exhibit a significantly longer
232 movement duration during SL-STS relative to normal STS, with movement duration becoming negatively
233 rather than positively correlated with strength for this adapted movement (Thongchoomsin et al 2020).
234 For these reasons, the SL-STS was chosen as the target movement in this study.

235

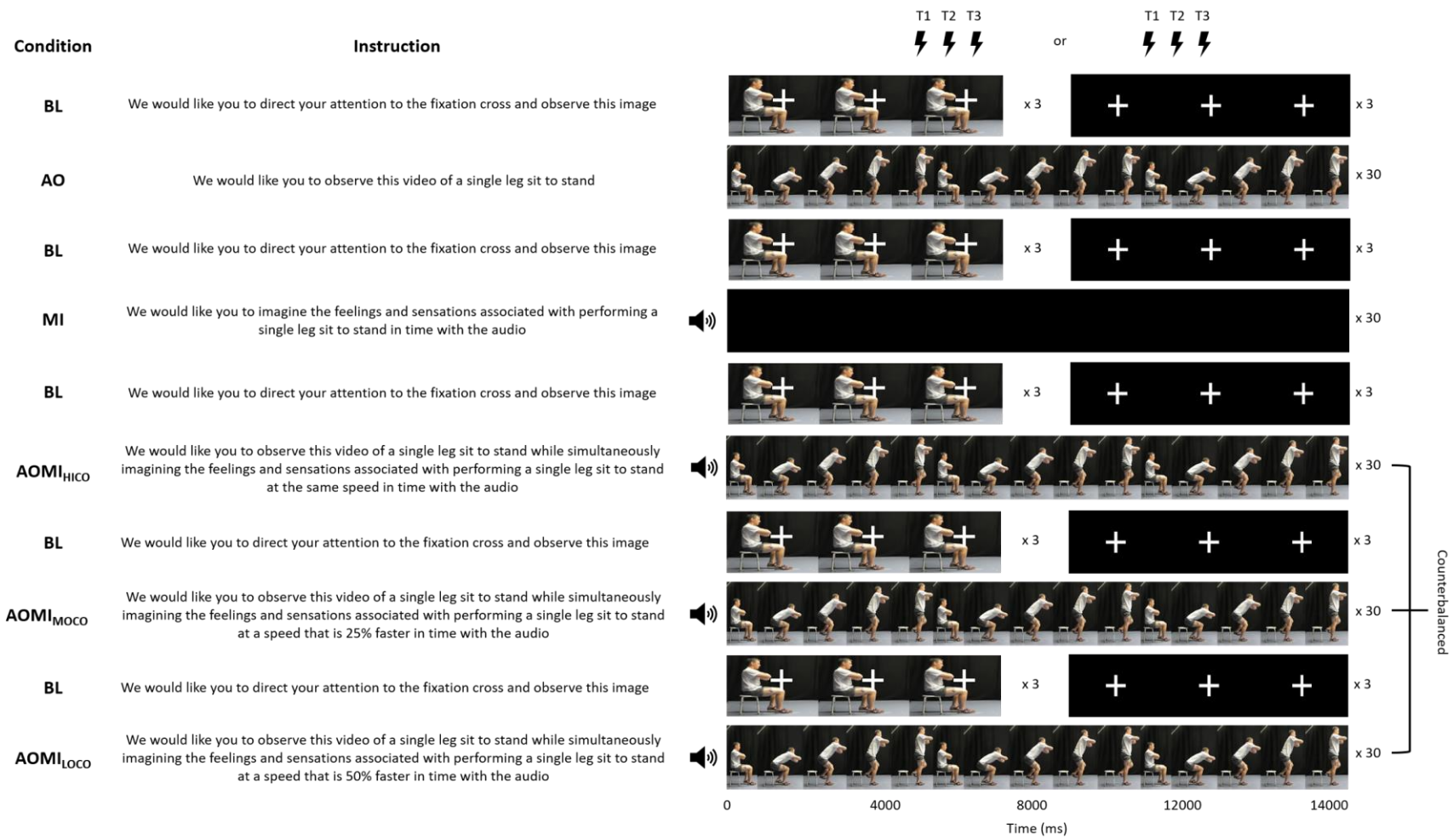

Figure 1. A Visual Representation of the Ten Experimental Blocks Completed During Each Testing Session. *Note:* The TMS was delivered at the point of peak EMG activity in the knee extensor muscle group for the models performing the *fast-paced* (T1), *medium-paced* (T2), and *slow-paced* (T3) SL-STS for either the second or third cycle of every AOMI trial, and at the same time point for trials in control conditions. The ordering of the TMS delivery was randomized and counterbalanced across trials for each experimental block. The model depicted in this figure is an author of this study.

242 **Stimuli Development**

243 Timings for the *slow-, medium-* and *fast-paced* SL-STS movements depicted in the video and
244 audio stimuli used in this study were determined through pilot testing given the novelty of the selected
245 target movement. Five pilot participants (4 male, 1 female) completed five successful trials of the SL-STS
246 under instructions to move (i) as slowly as possible (i.e., *slow-paced*), (ii) at a 'normal' pace (i.e.,
247 *medium-paced*), and (iii) as quickly as possible (i.e., *fast-paced*). During these trials, a marker on the C7
248 vertebra was tracked to identify movement start and end points using a 12-camera Vicon Vantage
249 motion capture system (Vicon, Oxford, UK) sampling at 100Hz. Surface electromyography (EMG) activity
250 was recorded for the vastus lateralis (VL), vastus medialis (VM) and rectus femoris (RF) quadricep
251 muscles using a single bipolar silver-chloride gel-electrode configuration on each muscle (2-cm diameter,
252 2-cm inter-electrode distance; Dual Electrode, Noraxon, Arizona, U.S.A.) to detect the point of peak EMG
253 activity for the *slow-*, *medium-* and *fast-paced* SL-STS movements. Quadricep muscles were selected as
254 the target muscles because they are a large contributor to forces during the STS (Ahmadi-Ahangar et al.,
255 2018; Miyoshi et al., 2005). On average across the pilot participants, the *slow-paced* SL-STS trial lasted
256 3.76 ± 1.23-s, the *medium-paced* SL-STS trial lasted 2.34 ± 0.38-s, and the *fast-paced* SL-STS trial lasted
257 1.69 ± 0.29-s. Since the average *medium-paced* SL-STS trial had a duration which was closer to the
258 duration of the *fast-paced* SL-STS trial, it was decided that the *medium-paced* SL-STS would be best
259 represented by the midpoint between the *slow* and *fast-paced* SL-STS (i.e., 2.73-s) .

260 Once the timings for the three SL-STS speeds were established, one male and one female model
261 were recruited for development of the video stimuli. The models were video recorded performing the
262 *slow-, medium-* and *fast-paced* SL-STS movement in the sagittal plane (see Figure 2) using a Panasonic
263 camera (HC-W570, 1920x1080 resolution and 50 frames per second). A metronome was used so that
264 both models could match the selected timings for all three movement speeds as closely as possible.
265 After reviewing footage captured for the models, the research team agreed upon each model's best trial

266 for the different SL-STS speeds by considering the time-discrepancy between the target and executed
267 trial durations, and the perceived smoothness of the executed SL-STS movement. The stimulation
268 timings were calculated based on the EMG data collected from the best trials of the two models. Using a
269 bespoke MATLAB (R2020a, The MathWorks) script, the peak EMG activity for each muscle at the three
270 different speeds was identified for both models. The absolute peak time was then determined and
271 normalized as a percentage of the total movement duration. These normalized values were averaged
272 across muscles for each speed and model. Movement durations for slow, medium, and fast speeds were
273 defined based on the slow movement duration, with the medium duration calculated as 75% of the slow
274 movement time and the fast duration defined as 50% of the slow movement time respectively for each
275 model. Finally, the stimulation times were derived by relating the average normalized peak activity to
276 these predefined durations (see https://osf.io/n7p2a for formula used). The calculated movement
277 duration times were used to produce movement sonification files on the open-source software Audacity
278 (Audacity Team version 2.4.1) to guide MI timing during conditions where this was required (i.e., the MI
279 control condition and three experimental conditions) in-line with the procedures of Castro and
280 colleagues (Castro, Bryjka, et al., 2021; Castro, Osman, et al., 2021).

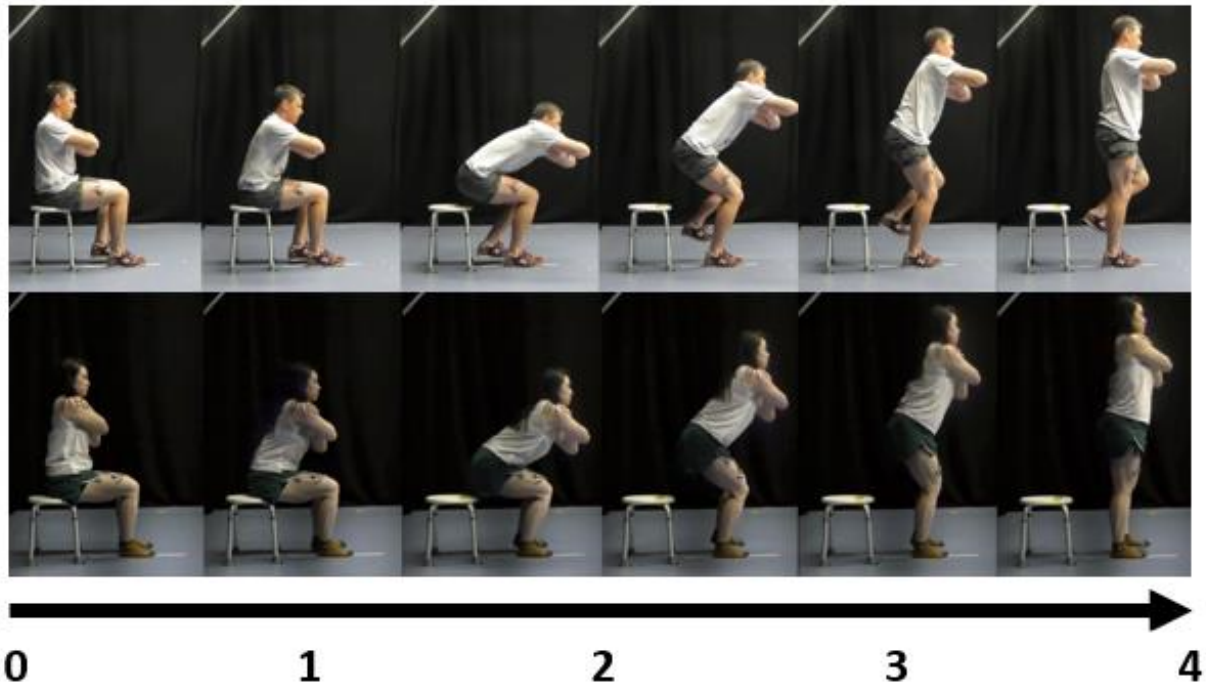

Figure 2. A visual depiction of the male (top) and female (bottom) models performing the *slow-paced* SL-STS used as the video stimuli in the AO control condition and AOMI experimental conditions used in this study. *Note:* The timing differed across the models, with the male model taking 3740ms and the female model taking 3660ms to complete the *slow-paced* SL-STS used in the video stimuli. The models depicted in this figure are both authors of this study.

Experimental Procedure

Surface Electromyography Preparation and Recording

Prior to EMG placement, the skin was prepared by shaving and cleaning the area where EMG electrodes were placed. The EMG system adopted for stimuli development was used to measure EMG activity for three KE muscles of the participants' right leg during the main experimental protocol. The EMG sensors (DTS-EMG sensors, Noraxon, USA) and electrodes were attached to the muscle belly of the target muscles based on the SENIAM (Hermens et al., 1999) guidelines. Noraxon wireless sensors (bandwidth of 20–450 kHz, 92 dB common mode rejection ratio and > 1015 Ω input impedance) transmitted the EMG signals to a desktop receiver (TeleMYO DTS EMG; Noraxon, Arizona, USA), and

296 these were sampled at 2 kHz via an analogue-to-digital convertor (Micro 1401–3) and desktop PC
297 utilizing Spike2 software (Cambridge Electronic Design, Cambridge, UK).

298 ***Transcranial Magnetic Stimulation Preparation***

299 **Optimal Scalp Position.** The TMS preparation procedures adhered to methodological guidelines,
300 as recorded via a methodological reporting checklist for TMS experiments (Chipchase et al., 2012) and
301 the methods employed in this study were adapted from established protocols (Grilc et al., 2024).
302 Participants were asked to wear a tight-fitting polyester cap with the center of the scalp (i.e., Cz),
303 defined by the intersection of lines from inion to nasion and from left to right tragus, measured and
304 marked as the top-right most corner of a 3x3cm grid drawn for identification of the optimal scalp
305 position (OSP). A single-pulse double-cone coil TMS (110 mm diameter) connected to a Magstim 200[2]
306 monophasic magnetic stimulator was originally placed at Cz and oriented to direct current flow from
307 anterior to posterior. The TMS coil was manually moved around the 3x3cm grid in 0.5cm intervals
308 posterior and lateral from Cz, and four stimulations were delivered at each site to identify the OSP that
309 produced the largest and most consistent MEP amplitudes across the three KE muscles. OSP sites ranged
310 from 0.5-2.5cm posterior and 0-1.5cm lateral to Cz, with the median OSP coordinates recorded as 1cm
311 posterior and 0.5cm lateral across the study sample.

312 **Resting Motor Threshold.** The resting motor threshold (RMT; excitability of the KE muscle
313 representation of the motor cortex at rest) was determined following the guidelines of Rossini et al.
314 (2015). This involved gradually reducing the stimulation intensity in 5% increments from the
315 participants' OSP intensity until five out of ten trials produced MEP amplitudes exceeding 50 µV in at
316 least two out of three KE muscles. Consistent with previous TMS literature on AOMI, the experimental
317 stimulation intensity was set at 110% of the RMT (Bruton et al., 2020; Grilc et al., 2024; Wright et al.,
318 2018) to minimize direct wave stimulation (Loporto et al., 2013). The mean RMT was 64 ± 11% and the
319 mean experimental stimulation intensity was 71 ± 12% of the maximum stimulator output, both similar

values to that of a recent TMS experiment investigating AOMI in lower-leg muscles (see Grilc et al., 2024).

Experimental Setup

The participants were seated comfortably on an isokinetic dynamometer chair (HUMAC NORM, CSMi, Stoughton, MA) in a dimly-lit Biomechanics Laboratory at the host university, with their upper body loosely strapped in place to reduce movement or repositions during the experimental block and maintain a consistent viewing position between blocks. The video stimuli were presented on an 80” adjustable screen (LED Interactive Multi-Touch Display, model 86GT-4K, SHENZHEN Hitevision Technology Co., Ltd.) placed 130cm directly in front of the participant (Figure 3) using DMASTR DMDX display software (Forster & Forster, 2003).

Figure 3. Experimental setup from two perspectives. The left image shows the experimenter positioning the TMS coil over the participant seated on the Cybex dynamometer, facing the screen. The right image offers an overhead view, approximating the participant's perspective with the coil in place. The people depicted in this figure are all authors of this study.

Familiarization

A familiarization phase was incorporated for all conditions where MI was instructed (i.e., MI, $AOMI_{HICO}$, $AOMI_{MOCO}$, $AOMI_{LOCO}$) to aid the participants' engagement with the upcoming experimental tasks. During this phase, participants watched five repetitions of a model performing the SL-STS at the required speed whilst seated on an adjustable stool with arms placed diagonally across their chest. After this, the participants physically practiced the movement for five repetitions, matching their speed to the speed of the model in the demonstration video. A further five physical repetitions were then completed,

342 with audio sonification added to the video of the model performing the SL-STS at the speed to be
343 imagined. The final step involved the participants receiving instructions to engage with MI of the SL-STS
344 in time with the audio sonification of the movement whilst being presented with a video of a *slow-paced*
345 SL-STS for the experimental conditions, or image of a blank screen for the MI condition.

346 ***Experimental Protocol***

347 The experimental protocol was repeated across two 3-hour testing sessions, at least 48 hours
348 apart. This design ensured the collection of sufficient data points for the study while minimizing
349 participant fatigue and discomfort. In each testing session, the participants completed ten experimental
350 blocks consecutively, with the five BL blocks lasting 90-s and the five main experimental blocks (i.e., AO,
351 MI, $AOMI_{HICO}$, $AOMI_{MOCO}$, $AOMI_{LOCO}$) lasting 450-s per block. A 180-srest period was included after each
352 of the main experimental blocks, and participants were encouraged to leave the testing chair to prevent
353 eye strain and muscular discomfort before familiarizing themselves with the stimuli and task for the next
354 experimental block. Prior to beginning the experiment, participants were asked to read the on-screen
355 instructions carefully, refrain from voluntary movement during the experimental blocks, and to attend
356 fully to the stimuli presented. Understanding of these instructions was verbally confirmed before the
357 start of each block. The 30-trial main experimental block incorporated a rest period after each set of 10
358 trials. Written and verbal reminders of the specific instructions for the condition were provided before
359 the participant completed each set of 10 trials. All trials were displayed on the LCD screen using
360 DMASTR DMDX display software (Forster & Forster, 2003) and lasted 10980ms for female participants
361 and 11220ms for male participants. For the AO control condition and three AOMI experimental
362 conditions (see Figures 1 and 2 for stimuli and instructions), the trials showed three repetitions of a
363 *slow-paced* SL-STS (3660ms per cycle for females, 3740ms per cycle for males). When observing the
364 *slow-paced* SL-STS, participants were instructed to simultaneously imagine the feelings and sensations
365 associated with a slow- ($AOMI_{HICO}$), *medium*- ($AOMI_{MOCO}$), or *fast-paced* SL-STS ($AOMI_{LOCO}$) using audio

366 sonification files lasting 100%, 75% and 50% of the *slow-paced* SL-STS duration for respective guidance.
367 For the MI condition, the participants observed a blank screen and engaged with MI following the same
368 instructions and audio sonification as the $AOMI_{HICO}$ condition.

369 ***TMS Data Collection***

370 Using a script run through Spike 2 software, a single TMS pulse was delivered once per trial
371 during the second (female = 3661-7320ms, male = 3741-7580ms) or third (female = 7321-10980ms,
372 male = 7581-11220ms) cycles of the observed *slow-paced* SL-STS movement used in the three
373 experimental and AO conditions, and at the corresponding time points for the trials for the BL and MI
374 control conditions. Participants were stimulated during two cycles of the SL-STS movement to reduce
375 the predictability of the stimulation and subsequent anticipatory behavior of the participants (Loporto
376 et al., 2012). TMS stimulation timepoints represented the point of peak EMG activity for the two models
377 when physically performing the different paced SL-STS trials used to produce the video and audio stimuli
378 for this study. TMS stimulation timepoints corresponding to the *fast*- (T1; female = 450ms, male = 550ms
379 after cycle onset), *medium*- (T2; female = 610ms, male = 720ms after cycle onset) and *slow-paced* SL-STS
380 (T3; female = 800ms, male = 1300ms after cycle onset) were randomly ordered and counterbalanced
381 within-conditions. A 3-s transition period was implemented between experimental trials to maintain an
382 inter-stimulus interval greater than 10-s to let the effects of the preceding TMS pulse diminish (Chen et
383 al., 1997).

384 ***Social Validation Data Collection***

385 Ratings of perceived MI ability were recorded using a 7-point Likert scale from 1 (*very easy to*
386 *feel*) to 7 (*very hard to fee*l) at the end of the familiarization phase, during the break periods between
387 each block of 10 trials, and at the end of the experiment for the conditions involving engagement with
388 MI processes (i.e., MI, $AOMI_{HICO}$, $AOMI_{MOCO}$, $AOMI_{LOCO}$). After finishing the TMS data collection for the
389 second testing session, participants recorded social validation data in a similar fashion to recent AOMI

experiments using TMS (e.g., Bruton et al., 2020; Grilc et al., 2024; Riach et al., 2018). Initially, participants recorded responses on a bespoke social validation questionnaire, where they rated perceived sex and ownership of the modeled SL-STS movements displayed in the conditions with an AO component (i.e., AO, $AOMI_{HICO}$, $AOMI_{MOCO}$, $AOMI_{LOCO}$) using three 5-point Likert scales from 1 (*totally disagree*) to 5 (*totally agree*). Participants then took part in a semi-structured social validation interview designed to understand their experiences across the different conditions and check for compliance with the intended manipulations.

Data Analysis

TMS Data Processing

Peak-to-peak MEP amplitudes were recorded from three KE muscles (VM, VL and RF) of the participants' right leg on a trial-by-trial basis and averaged across all successful trials for T1, T2 and T3 TMS stimulation timepoints per condition from both testing sessions. After extracting the data from Spike 2, and separating the data based on TMS stimulation timepoint, a two-part screening process was used to determine successful trials. First, trials were screened for the presence of an MEP response, and any trials that did not evoke an MEP amplitude of sufficient magnitude (i.e., 50 µV) were removed. It is well-established that MEP amplitudes are increased for a target muscle if the EMG activity in that muscle is above resting state levels at, or immediately prior to, the time of TMS stimulation (Devanne et al., 1997; Hess et al., 1987). To control for this, EMG activity was recorded for 200 ms prior to the delivery of each TMS pulse and any trials where the EMG amplitude exceeded normal baseline values (mean ± 2.5 SD) for that TMS stimulation timepoint and condition were removed (e.g., Riach et al., 2018; Wright et al., 2014; 2018). For the study sample, a mean value of 4.71 (± 3.93) trials for the VM muscle, 6.66 (± 6.05) trials for the VL muscle, and 2.35 (± 2.59) trials for the RF muscle were removed per TMS stimulation timepoint and condition. This resulted in the sample having a mean value of 19.22 (± 4.69) trials with an uncontaminated MEP response in one or more KE muscles, providing a reliable estimate of

414 CSE per TMS stimulation timepoint and condition (Cuypers et al., 2014). On a muscle-by-muscle basis,
415 the raw MEP amplitude data for successful trials was normalized using a *z*-score transformation to
416 account for the large intra- and inter-participant variability in MEP amplitudes at rest (e.g., Bruton et al.,
417 2020; Grilc et al., 2024; Wright et al., 2014). For each participant, this procedure involved standardizing
418 the MEP amplitude value recorded for each successful trial against all other MEP amplitude values
419 recorded for successful trials for that TMS stimulation timepoint across the two testing sessions. The
420 mean amplitude for all successful trials at each TMS stimulation timepoint (i.e., T1, T2, T3) was
421 represented by a value of zero, and values for each condition were denoted by how many standard
422 deviations that condition was above or below the mean of all conditions. Once the *z*-score
423 transformation was complete, the mean *z*-score MEP amplitude value was recorded for the three KE
424 muscles on a trial-by-trial basis. This mean was calculated from three KE muscles for 70.41%, two KE
425 muscles for 19.83%, and one KE muscle for 9.76% of successful trials. For all participants, a mean *z*-score
426 MEP amplitude value was calculated per condition at each TMS stimulation timepoint for analysis.

427 ***TMS Data Analysis***

428 The *z*-score MEP amplitude data for the KE muscles was normally distributed at each TMS
429 stimulation timepoint, permitting the use of analysis of variance (ANOVA) statistical tests. Three
430 separate one-way repeated measure ANOVA tests with six levels (Condition: BL, AO, MI; $AOMI_{HICO}$;
431 $AOMI_{MOCO}$; $AOMI_{LOCO}$) were run using the rstatix package (Kassambara, 2023) and the data was visualized
432 using the ggplot2 package (Wickham, 2016) in R studio statistical software (version 4.3.2). Bonferroni
433 contrasts were used for post-hoc pairwise comparisons. Outlier analysis was conducted using
434 interquartile range values, and data points identified as outliers were removed from the three ANOVA
435 analyses (T1 = 2, T2 = 2, T3 = 3 outliers). To test for a potential ordering effect across the experiment, a
436 one-way repeated measure ANOVA test with five levels (BL block: block 1, block 3, block 5, block 7, block
437 9) was conducted for *z*-score MEP amplitude data recorded in BL experimental blocks. For this

comparison, the *z*-score transformation was conducted based on the data from the 60 BL trials collected across the two testing sessions. A one-way repeated measures ANOVA analysis performed on the BL condition *z*-score MEP amplitude data revealed no significant main effect of block, $F_{(4, 72)} = 1.01$, $p = .41$, $\eta_p^2 = .05$.

Social Validation Data Analysis

A one-way repeated measures ANOVA with four levels (Condition: MI; $AOMI_{HICO}$; $AOMI_{MOCO}$; $AOMI_{LOCO}$) was run on the perceived MI ability data collected from the social validation questionnaire to investigate differences across the conditions with MI processes. An independent samples t-test (Participant Sex: male; female) was run on the perceived body ownership, masculinity, and femininity data collected from the social validation questionnaire to investigate differences in male and female participants' ratings of the movements displayed across the conditions with AO processes. Interview data was transcribed, coded, and grouped on a question-by-question basis to offer detailed explanations for the MI ability ratings from the social validation questionnaire.

Results

MEP Amplitude Data

One-way repeated measures ANOVA analyses performed on the *Z*-score MEP amplitude data revealed a significant large main effect of condition at T1, $F_{(5, 90)} = 8.28$, $p < .001$, $\eta_p^2 = .31$, T2, $F_{(3.04, 54.69)} = 8.32$, $p < .001$, $\eta_p^2 = .31$, and T3, $F_{(5, 85)} = 18.4$, $p < .001$, $\eta_p^2 = .51$, TMS stimulation timepoints. Post-hoc pairwise comparisons between the experimental conditions (i.e., $AOMI_{HICO}$, $AOMI_{MOCO}$, $AOMI_{LOCO}$) and control conditions (i.e., BL, AO, MI) across the three TMS stimulation timepoints are reported below.

Highly-Coordinated AOMI ($AOMI_{HICO}$)

Post-hoc pairwise comparisons at T3 (Figure 4), the TMS stimulation timepoint corresponding to the *slow-paced* SL-STS, showed that *Z*-score MEP amplitudes were significantly larger in the $AOMI_{HICO}$ condition compared to the BL ($p < .001$) and AO ($p < .001$) conditions, but not the MI condition ($p = .29$).

Post-hoc pairwise comparisons at T2 (Figure 5), the TMS stimulation timepoint corresponding to the *medium-paced* SL-STS, showed no significant differences between the $AOMI_{HICO}$ condition and the three control conditions (*p*s > .05). Post-hoc pairwise comparisons at T1 (Figure 6), the TMS stimulation timepoint corresponding to the *fast-paced* SL-STS, showed that *Z*-score MEP amplitudes were significantly larger in the $AOMI_{HICO}$ condition compared to the BL ($p = .01$) and AO ($p < .001$) conditions, but not the MI condition ($p = .34$).

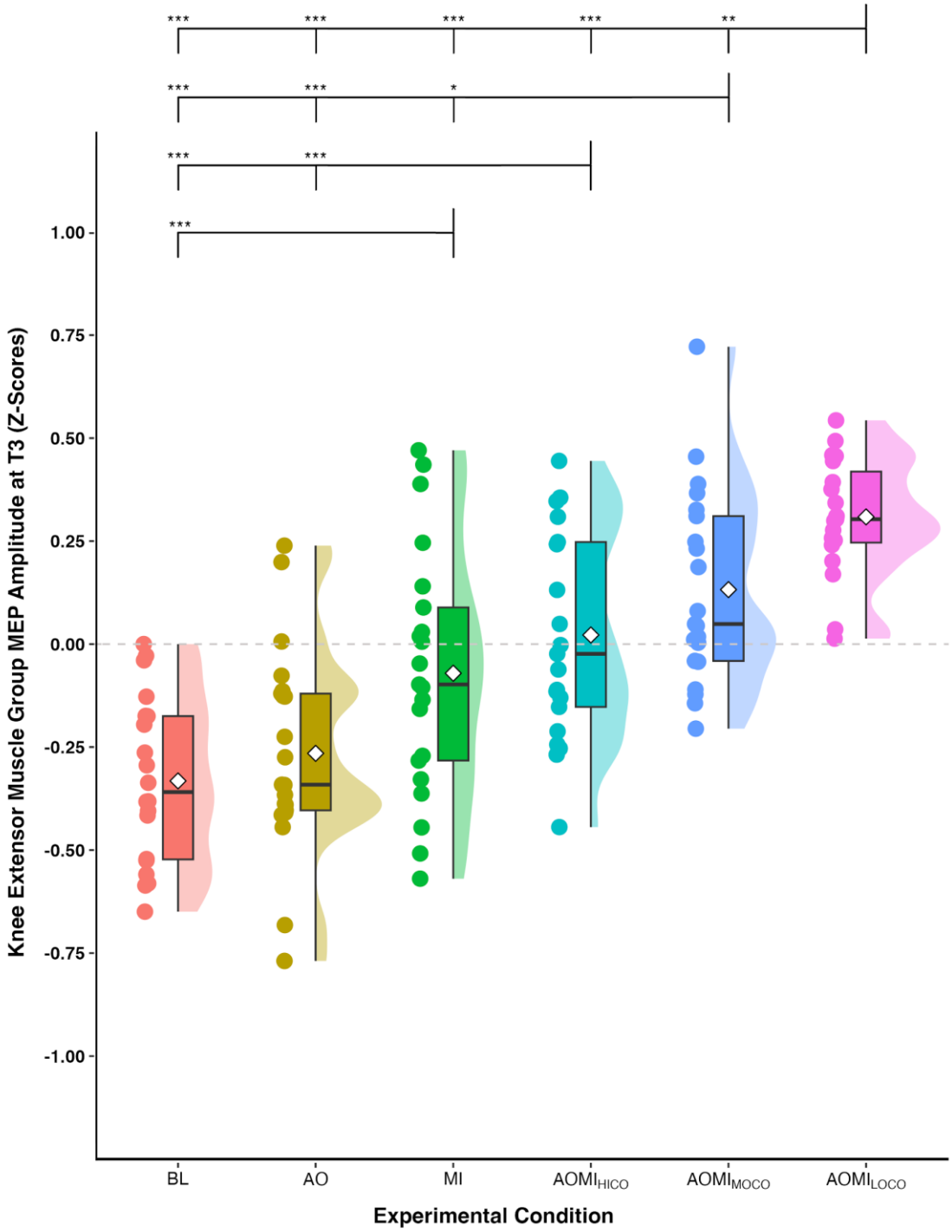

Figure 4. Box and violin plot with raw data points displaying z-score normalized MEP amplitudes from the knee extensor muscle group at the stimulation timepoint corresponding to the *slow-paced* SL-STS (T3) for the three control and three experimental conditions. *Note:* Thick horizontal black lines represent the median average and white diamonds represent the mean average for each box plot. Individual participant data points are represented by circular markers. BL – baseline; AO – action observation; MI – motor imagery; AOMI$_{HICO}$ – highly-coordinated action observation and motor imagery; AOMI$_{MOCO}$ – moderately-coordinated action observation and motor imagery; AOMI$_{LOCO}$ – lowly-coordinated action observation and motor imagery; *$p < .05$, **$p < .01$, ***$p < .001$.

Moderately-Coordinated AOMI ($AOMI_{MOCO}$)

Post-hoc pairwise comparisons at T2 (Figure 5), the TMS stimulation timepoint corresponding to the *medium-paced* SL-STS, showed that *Z*-score MEP amplitudes were significantly larger in the $AOMI_{MOCO}$ condition compared to the BL ($p = .01$) and AO ($p = .02$) conditions, but not the MI condition ($p = .07$). Post-hoc pairwise comparisons at T3 (Figure 4), the TMS stimulation timepoint corresponding to the *slow-paced* SL-STS, showed that *Z*-score MEP amplitudes were significantly larger in the $AOMI_{MOCO}$ condition compared to the BL ($p < .001$), AO ($p < .001$) and MI ($p = .02$) conditions. Post-hoc pairwise comparisons at T1 (Figure 6), the TMS stimulation timepoint corresponding to the *fast-paced* SL-STS, showed that Z-score MEP amplitudes were significantly larger in the $AOMI_{MOCO}$ condition compared to the BL ($p = .04$) and AO ($p = .01$) conditions, but not the MI condition ($p = .56$).

Lowly Coordinated-AOMI ($AOMI_{LOCO}$)

Post-hoc pairwise comparisons at T1 (Figure 6), the TMS stimulation timepoint corresponding to the *fast-paced* SL-STS, showed that *Z*-score MEP amplitudes were significantly larger in the $AOMI_{LOCO}$ condition compared to the BL ($p < .001$), AO ($p < .001$), and MI conditions ($p < .001$). Post-hoc pairwise comparisons at T2 (Figure 5), the TMS stimulation timepoint corresponding to the *medium-paced* SL-STS, showed that *Z*-score MEP amplitudes were significantly larger in the $AOMI_{LOCO}$ condition compared to the BL ($p = .01$), AO ($p = .01$), and MI conditions ($p = .02$). Post-hoc pairwise comparisons at T1 (Figure 6), the TMS stimulation timepoint corresponding to the *slow-paced* SL-STS, showed that *Z*-score MEP amplitudes were significantly larger in the $AOMI_{LOCO}$ condition compared to the BL ($p < .001$), AO ($p < .001$), and MI conditions ($p < .001$).

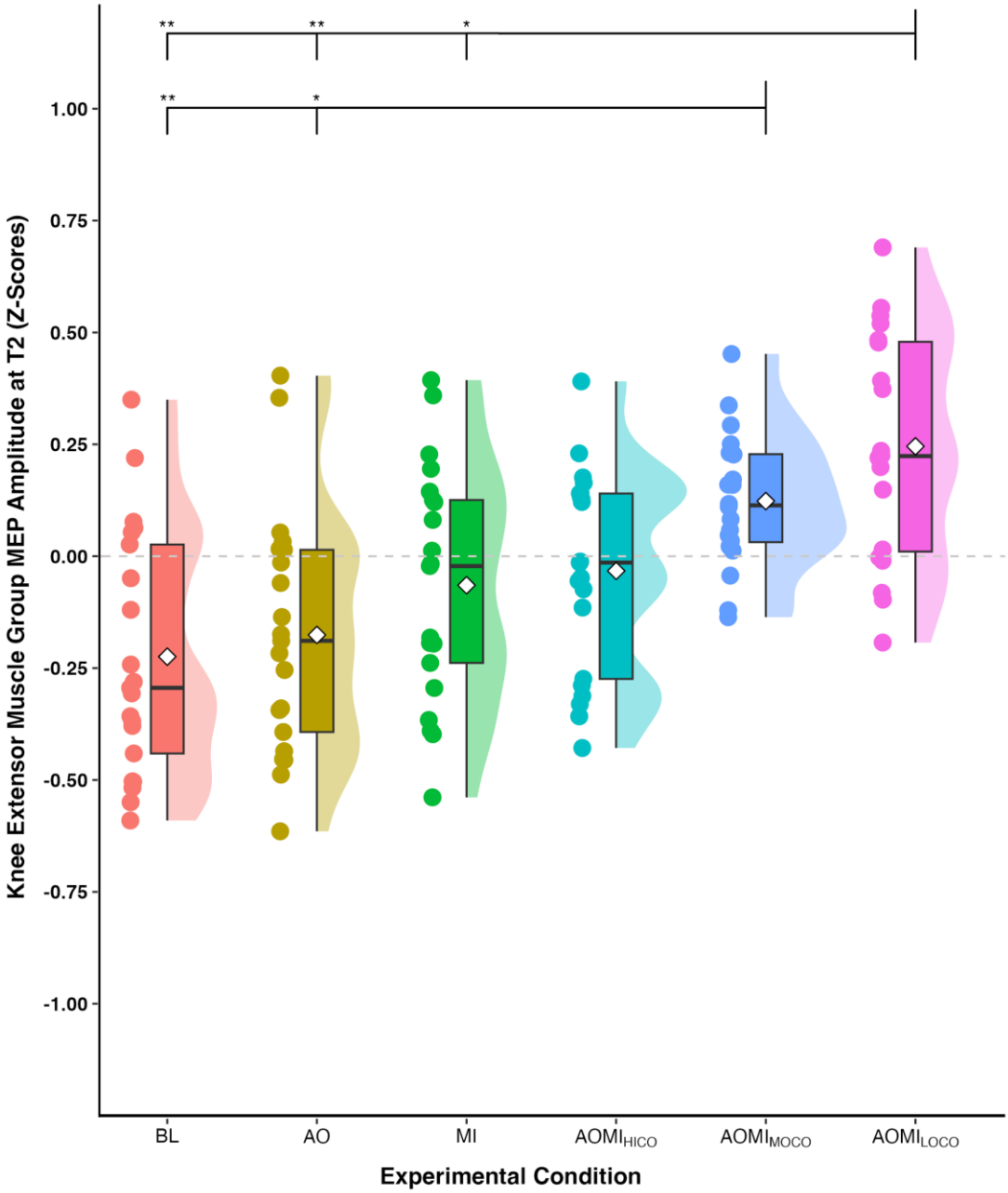

Figure 5. Box and violin plot with raw data points displaying z-score normalized MEP amplitudes from the knee extensor muscle group at the stimulation timepoint corresponding to the *medium-paced* SL-STS (T2) for the three control and three experimental conditions. *Note:* Thick horizontal black lines represent the median average and white diamonds represent the mean average for each box plot. Individual participant data points are represented by circular markers. BL – baseline; AO – action observation; MI – motor imagery; AOMI$_{HICO}$ – highly-coordinated action observation and motor imagery; AOMI$_{MOCO}$ – moderately-coordinated action observation and motor imagery; AOMI$_{LOCO}$ – lowly-coordinated action observation and motor imagery; *$p < .05$, **$p < .01$.

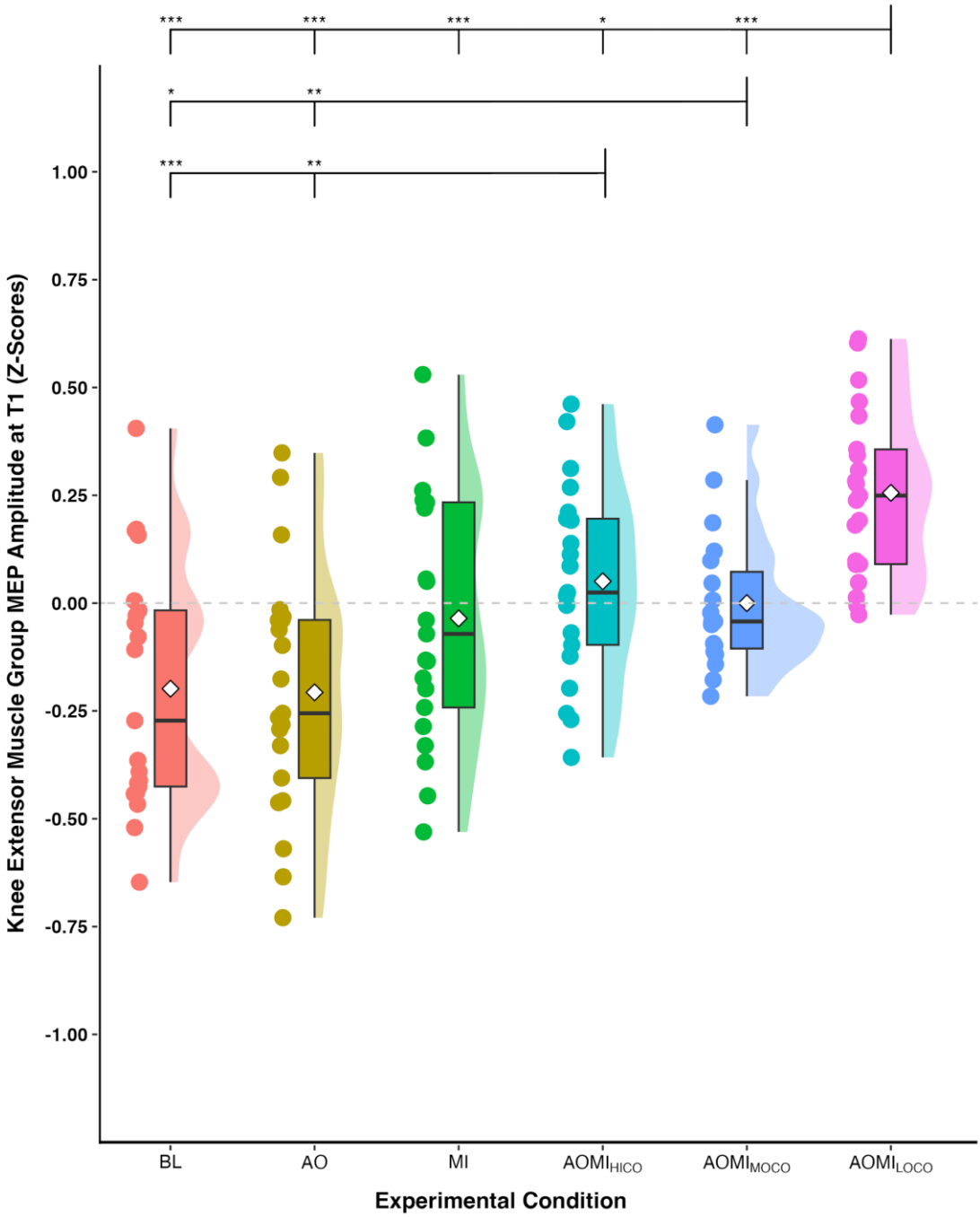

Figure 6. Box and violin plot with raw data points displaying z-score normalized MEP amplitudes from the knee extensor muscle group at the stimulation timepoint corresponding to the *fast-paced* SL-STS (T1) for the three control and three experimental conditions. *Note:* Thick horizontal black lines represent the median average and white diamonds represent the mean average for each box plot. Individual participant data points are represented by circular markers. BL – baseline; AO – action observation; MI – motor imagery; AOMI$_{HICO}$ – highly-coordinated action observation and motor imagery; AOMI$_{MOCO}$ – moderately-coordinated action observation and motor imagery; AOMI$_{LOCO}$ – lowly-coordinated action observation and motor imagery; *$p < .05$, **$p < .01$, ***$p < .001$.

516 **Social Validation Data**

517 **Questionnaire Responses**

518 A one-way repeated measures ANOVA analysis performed on the perceived MI ability data
519 revealed a significant effect of condition $F_{(3, 60)} = 14.23$, $p < .001$, $\eta_p^2 = .14$. Post-hoc pairwise
520 comparisons showed that perceived MI ability scores were significantly larger in the $AOMI_{HICO}$ condition
521 compared to the MI ($p < .001$), $AOMI_{MOCO}$ ($p < .001$), and $AOMI_{LOCO}$ ($p < .001$) conditions. All participants
522 felt like they were looking at a same-sex model, with male participants recording a mean response of
523 1.67 (±0.50) indicating total agreement that the model they watched was male, and female participants
524 recording a mean response of 1.83 (±0.41) indicating total agreement that the model they watched was
525 female. Despite the acknowledgement that the models were the same-sex as the participants, only six
526 participants (28.57%) felt like they were watching their own performance of the *slow-paced* SL-STS.

527 ***Interview Responses***

528 The interview data provided additional detail about the preferences and strategies adopted by
529 the participants across the experimental conditions. Participants provided mixed responses about
530 perceived MI ability across the conditions where MI was instructed. Sixteen participants (76.19%)
531 suggested MI was easiest in the $AOMI_{HICO}$ condition, with most participants outlining that the synchrony
532 between the observed video and the audio sonification of the SL-STS reduced the difficulty of the
533 cognitive task and facilitated their imagery of the movement (e.g., "It was playing at the correct speed,
534 so I didn't even need to do that [synchronize], so all my attention could be focused on imagining the
535 feeling and sensations" [participant 3]). Conversely, thirteen participants (61.90%) indicated that MI was
536 most difficult in the $AOMI_{MOCO}$ condition and eight participants (38.10%) reported that $AOMI_{LOCO}$ was the
537 most challenging condition in terms of MI ability. Participants who found MI most difficult during
538 $AOMI_{MOCO}$ noted that the close overlap between the speed of the AO and MI processes made it harder
539 to time and maintain the imagined *medium-paced* SL-STS (e.g., "I think the one where I imagined the

middle speed with the slow video [$AOMI_{MOCO}$], that was a bit challenging. Maybe because the speeds were much closer as well, so it's a bit more challenging to imagine, to make sure that I'm not slowing the image to match the video" [participant 12]). In a somewhat contradictory manner, participants who found MI most difficult during $AOMI_{LOCO}$ suggested the scale of the difference between AO and MI processes, and the sheer speed of the imagery, made it hard to accurately generate the imagined *fast-paced* SL-STS (e.g., "I found that one the hardest because it was too distanced between the two [observed and imagined movements] and it was negatively impacting the movements I was imagining due to the mixed signals" [participant 5]).

All participants confirmed that they could successfully engage with MI when instructed to across the experiment. Fourteen participants (66.67%) stated that their MI consisted of only kinesthetic aspects for all conditions (e.g., “there's [imagining] the initial sort of force production bit, which is really tight on the quadriceps, and then once you're sort of almost fully extended, that's when [imagining] the feelings of being balanced comes into it." [participant 3]). However, seven participants (33.33%) indicated that they sometimes generated visual images as well as kinesthetic images of the SL-STS, with this largely taking place in the MI condition due to a lack of visual stimuli, or in the AOMI conditions when attempting to reset their timing or attention to the task. Of these, three participants (14.29%) imagined seeing her/himself performing the SL-STS from a first-person visual perspective whilst maintaining kinesthetic imagery (e.g., "That [third-person] is the perspective I have of that person doing it [in the video], but not of me doing it, because I'm not on the outside of me, so I imagine seeing and feeling it as if I'm practicing" [participant 7]). Four participants (19.05%) imagined seeing her/himself performing the SL-STS from a third-person alongside their kinesthetic imagery (e.g., "There were probably moments where I was imagining things from a sagittal plane as the video was showing, but I think a lot of the time my focus was on imagining the feeling of and the kind of sensations involved” [participant 16]).

564 **Discussion**

565 This study aimed to test the DASH (Eaves, Riach, et al., 2016) and VGH (Meers et al., 2020)
566 propositions for *coordinative* AOMI by comparing CSE responses during highly-, moderately-, and lowly-
567 coordinated AOMI for a SL-STS movement. Task-related MI ability and social validation data were also
568 collected to help explain the cognitive processes underpinning any differences in CSE response during
569 these different types of *coordinative* AOMI. CSE was facilitated for $AOMI_{HICO}$ at T3, indicating a combined
570 effect for the observed and imagined *slow-paced* SL-STS. CSE was facilitated for the $AOMI_{MOCO}$ condition
571 at T3 and T2, indicating an effect for the observed *slow-paced* SL-STS and the imagined *medium-paced*
572 SL-STS, respectively. CSE was facilitated for $AOMI_{LOCO}$ at T3 and T1, indicating an effect for the observed
573 *slow-paced* SL-STS and the imagined *fast-paced* SL-STS. However, CSE was facilitated for $AOMI_{MOCO}$ and
574 $AOMI_{LOCO}$ at all three timepoints, $AOMI_{LOCO}$ reported the greatest CSE facilitation at all three timepoints,
575 and facilitation was inversely related to the level of coordination for AOMI at T3 and T2. These findings
576 suggest the increased speed of MI drove the facilitation in CSE across the study as a whole. Overall, the
577 findings lend possible support to both the DASH and VGH propositions for *coordinative* AOMI, as
578 discussed below.

579 In this experiment, $AOMI_{HICO}$ involved the simultaneous observation and imagery of a *slow-*
580 *paced* SL-STS movement. Our findings align with both the DASH (Eaves, Riach, et al., 2016) and VGH
581 (Meers et al., 2020) propositions for $AOMI_{HICO}$ as CSE facilitation was increased for this condition at T3,
582 the stimulation timepoint at which the observed and imagined aspects were incongruence for the
583 observed and imagined *slow-paced* SL-STS, compared with BL and AO, but not MI control conditions.
584 This finding agrees with a body of literature showing CSE facilitation for $AOMI_{HICO}$ relative to control and
585 independent AO conditions (e.g., Bruton et al., 2020; Grilc et al., 2024; Wright et al., 2018). Based on the
586 propositions of the DASH (Eaves, Riach, et al., 2016), the CSE facilitation reported for $AOMI_{HICO}$ is caused
587 by the two motor representations for AO and MI of the *slow-paced* SL-STS merging as one sensorimotor

588 stream, leading to widespread activity in the premotor cortex. This merger is likely to cause increased
589 activity in overlapping brain regions for AO and MI, whilst also increasing activity across a wider neural
590 network that involves brain areas solely recruited during AO and MI for the *slow-paced* SL-STS during
591 $AOMI_{HICO}$ (Hardwick et al., 2018; Filimon et al., 2015). An alternative explanation is provided by the VGH
592 (Meers et al., 2020), which argues that the CSE facilitation during $AOMI_{HICO}$ is indicative of a stronger
593 motor representation for MI of the *slow-paced* SL-STS due to the priming effect of AO for the same *slow-*
594 *paced* SL-STS. The social validation data lends support to this assertion, as participants reported
595 significantly greater MI ability during the $AOMI_{HICO}$ condition compared to all other conditions where MI
596 was instructed in this experiment. Participants reasoned that MI was easier in this condition due to the
597 synchrony between the video demonstration and sonification of the *slow-paced* SL-STS, indicating that
598 the MI component took priority during $AOMI_{HICO}$. In line with the findings of a recent meta-analysis
599 (Chye et al., 2022), CSE facilitation at T3 was descriptively, but not significantly greater for $AOMI_{HICO}$
600 compared with MI of the *slow-paced* SL-STS. In combination, our CSE and social validation data support
601 the propositions of the VGH that MI is primed during $AOMI_{HICO}$, but indicate that this effect might be
602 minimal, at least for complex whole-body actions like the *slow-paced* SL-STS used in this study.
603 In the current study, $AOMI_{MOCO}$ involved the observation of a *slow-paced* SL-STS and
604 simultaneous imagination of the feelings and sensations involved with a *medium-paced* SL-STS. Our
605 findings align with the DASH (Eaves, Riach, et al., 2016) proposition for *coordinative* AOMI as CSE was
606 facilitated for the $AOMI_{MOCO}$ condition at T3 compared with all three control conditions indicating an
607 effect for the observed *slow-paced* SL-STS, and at T2 compared with BL and AO control conditions
608 indicating an effect for the imagined *medium-paced* SL-STS. This finding is similar to that reported by
609 Bruton et al. (2020) who showed CSE facilitation for both observed and imagined muscles when
610 controlling for visual attention during *coordinative* AOMI of finger movements, but disagrees with the
611 findings of Meers et al. (2020) and Grilc et al. (2024) that showed CSE facilitation for imagined muscles

612 only during *coordinative* AOMI of finger movements and lower-limb movements, respectively. Based on
613 the propositions of the DASH, the requirement to co-represent two related, but not identical,
614 movements during *coordinative* AOMI involves the maintenance of two parallel sensorimotor
615 representations for the observed *slow-paced* SL-STS and imagined *medium-paced* SL-STS as a set of
616 action affordances. The findings for $AOMI_{MOCO}$ in this study indicate that it is possible to simultaneously
617 co-represent two variations of the same SL-STS movement that differ based on the speed (i.e., *slow*- vs.
618 *medium-paced*) of the simulated movement.

619 The social validation questionnaire and interview data collected in this study indicated that
620 participants found it difficult to both observe the *slow-paced* and imagine the *medium-paced* SL-STS
621 movements during the $AOMI_{MOCO}$ condition because of the close overlap between the speed of the
622 movements. Based on the propositions of the VGH (Meers et al., 2020), the imagined *medium-paced* SL-
623 STS is prioritized during $AOMI_{MOCO}$, meaning the motor representation is only maintained for this action
624 and the observed *slow-paced* SL-STS serves as a visual guide to facilitate MI processes. If this proposition
625 held true, CSE would only be facilitated at T2 during $AOMI_{MOCO}$, as per recent findings (Grilc et al., 2024;
626 Meers et al., 2020). This was not the case, as CSE facilitation was increased at both T3 and T2 for this
627 condition, a finding that could be explained by attentional mechanisms underlying engagement with
628 $AOMI_{MOCO}$. It is possible that participants directed their attention towards either the observed or
629 imagined SL-STS movements when engaging in $AOMI_{MOCO}$ to account for the cognitive demands of the
630 task, and support the generation and maintenance of imagery as the effortful form of movement
631 simulation. Indeed, eye movement (Bruton et al., 2020) and electroencephalographic data (Eaves,
632 Behmer et al., 2016) shows that individuals switch their attention between observed and imagined
633 actions during *coordinative* AOMI. The interview findings reported here are consistent with this
634 interpretation, suggesting participants may direct more attention to either the observed or imagined
635 action on a trial-by-trial basis, resulting in CSE facilitation at T2 and T3 when aggregated across the

636 $AOMI_{MOCO}$ condition in-full. It is noteworthy that CSE facilitation is increased for $AOMI_{MOCO}$ compared
637 with AO at both T2 and T3, and MI at T3, suggesting an additive effect beyond AO or MI processes in
638 isolation. This is indicative of co-representation of the two related, but not identical, movements during
639 $AOMI_{MOCO}$ and disagrees with the proposition that MI drives the CSE facilitation resulting from
640 *coordinative* AOMI (Grilc et al., 2024; Meers et al., 2020).

641 In the $AOMI_{LOCO}$ condition used in this study, participants observed a *slow-paced* SL-STS and
642 simultaneously imagined the feelings and sensations involved with a *fast-paced* SL-STS. Our findings
643 disagree with the propositions of both the DASH (Eaves, Riach, et al., 2016) and VGH (Meers et al., 2020)
644 accounts for *coordinative* AOMI as CSE was facilitated for the $AOMI_{LOCO}$ condition at T3 and T1 compared
645 with all other conditions, indicating an effect for both the observed *slow-paced* and imagined *fast-paced*
646 SL-STS during $AOMI_{LOCO}$. This finding contrasts most TMS findings on *coordinative* AOMI, as studies have
647 typically reported increased CSE facilitation for the imagined but not the observed action (Grilc et al.,
648 2024; Meers et al., 2020). Given the low coordination between the movement speeds used for AO and
649 MI components of $AOMI_{LOCO}$, the results also warrant comparison with *conflicting* AOMI. In the only TMS
650 study employing a *conflicting* AOMI condition, Bruton et al. (2020) reported no increase in CSE
651 facilitation in the observed and imagined muscles compared to control conditions (BL, AO). The authors
652 also showed that CSE facilitation was increased in the simultaneously observed and imagined muscle
653 during *congruent* AOMI, and imagined muscle during *coordinative* AOMI, when compared to the
654 *conflicting* AOMI condition. This suggests that the $AOMI_{LOCO}$ condition employed in this study is more
655 representative of *coordinative* than *conflicting* AOMI, but this does not explain the facilitation of CSE for
656 both the observed and imagined SL-STS movements during this condition. It is possible that this reflects
657 the maintenance of two parallel sensorimotor streams for the observed and imagined actions, even
658 when there is a sizable temporal discrepancy between the observed and imagined actions during
659 $AOMI_{LOCO}$, aligning with the sentiments of the DASH (Eaves, Riach et al., 2016).

660 An alternative explanation, consistent with the VGH (Meers et al., 2020), is that MI is driving the
661 increased CSE facilitation reported for $AOMI_{LOCO}$ at all three stimulation timepoints. The level of force or
662 effort of an imagined task is represented in corticomotor activity, with higher force/effort demands
663 leading to increased CSE facilitation during MI (e.g., Helm et al., 2015; Tatemoto et al., 2017; Tremblay
664 et al., 2001). In this study, CSE increased as imagery speed increased during *coordinative* AOMI for T2
665 and T3, and the condition that required the participants to imagine performing the fastest SL-STS (i.e.,
666 $AOMI_{LOCO}$) had the greatest CSE facilitation across all three stimulation timepoints. It was expected that
667 $AOMI_{LOCO}$ would lead to CSE facilitation at T1, as this is the stimulation timepoint aligned to peak EMG
668 activity for a physically executed *fast-paced* SL-STS. CSE facilitation at T2 and T3 was not expected for
669 this experimental condition. Able imagers demonstrate smaller time differences, known as mental
670 chronometry, between physical performance and MI trials of the same task (Guillot & Collet, 2005). This
671 is logical given the shared neural pathways for movement execution and movement simulation
672 (Hardwick et al., 2018), but more difficult movement tasks typically lead to greater temporal
673 discrepancies between imagined and executed movements (Guillot & Collet, 2005). The social validation
674 data indicated that participants perceived their imagery ability to be lowest during $AOMI_{LOCO}$, with the
675 conflicting speeds for the observed *slow-paced* and imagined *fast-paced* SL-STS movements disrupting
676 their imagery. Despite the use of audio sonification to guide MI during *coordinative* AOMI in this study
677 (Castro, Bryjka, et al., 2021; Castro, Osman, et al., 2021) it is possible that participants timing of the
678 imagery was delayed across some trials for the $AOMI_{LOCO}$ condition due to the complexity of the task,
679 possibly explaining the increased CSE facilitation across all three stimulation timepoints for this form of
680 *coordinative* AOMI.

681 The findings reported for different forms of *coordinative* AOMI in this study have important
682 implications for motor (re)learning in sports and rehabilitation settings. $AOMI_{HICO}$ is recommended as the
683 optimal form of motor simulation because it addresses the limitations involved with AO (e.g., directs the

684 attention of the learner) or MI (e.g., provides visual movement information to support the generation
685 and maintenance of kinesthetic images) when used alone, and has additive benefits towards motor skill
686 performance compared to these techniques in isolation (Chye et al., 2022; Wright et al., 2022). These
687 performance benefits are supposedly underpinned by synaptic plasticity processes similar to those
688 observed during physical practice (Holmes & Calmels, 2008). The two other types of *coordinative* AOMI
689 employed in this study ($AOMI_{MOCO}$, $AOMI_{LOCO}$) facilitated CSE at stimulation timepoints aligned with the
690 observed and imagined movements. They may therefore have the capacity to benefit (re)learning of
691 variations of the same action or joint actions (Vogt et al., 2013). These *coordinative* AOMI conditions are
692 a viable complementary training method to physical therapy in rehabilitation settings and could be used
693 to promote the (re)learning of actions that are currently impaired or missing from a person's motor
694 repertoire. For example, a post-stroke patient may benefit from observing videos of themselves
695 accurately performing leg movements such as the SL-STS with their non-affected limb, whilst
696 simultaneously imagining the feelings and sensations associated with performing the same or similar leg
697 movements at different speeds with their impaired limb (e.g., McCormick et al., 2022). In such cases,
698 $AOMI_{MOCO}$ and $AOMI_{LOCO}$ could support motor (re)learning by promoting Hebbian plasticity in a similar
699 manner to that described above for $AOMI_{HICO}$.

700 All four studies investigating *coordinative* AOMI have used TMS to examine the
701 neurophysiological mechanisms underpinning this form of action simulation (see Bruton et al., 2020;
702 Grilc et al., 2024; Meers et al., 2020; this study), yet behavioral research is lacking. There is a need to
703 empirically test the effectiveness of $AOMI_{MOCO}$ and $AOMI_{LOCO}$ as movement interventions across
704 populations and contexts in order to substantiate propositions that these types of *coordinative* AOMI
705 may be better than $AOMI_{HICO}$ for (re)learning variations of the same movement or joint actions where
706 interpersonal coordination is required (Eaves et al., 2022). Longitudinal research incorporating both
707 neurophysiological and behavioral measures is required to verify the extent to which repeated

engagement in different types of *coordinative* AOMI promotes functional connectivity and plasticity changes within the brain, and the association between these neural adaptations and any motor performance and learning improvements after a *coordinative* AOMI intervention period (Bruton et al., 2020; Chye et al., 2022; Grilc et al., 2024).

Single-pulse TMS permits time- and muscle-specific measurement of CSE facilitation (Naish et al., 2014; Rothwell, 1997), and thus allowed the contributions of each simulation state (i.e., the observed and imagined actions) to be distinguished by examining the effects of different types of *coordinative* AOMI on MEP responses in the KE muscle group at three stimulation timepoints. However, this study was limited by only recording MEPs from the lower limb muscles (i.e., the KE muscle group) for the SL-STS during the different *coordinative* AOMI conditions. Future studies should topographically map and record EMG from a wider selection of whole body musculature to draw more conclusive evidence regarding CSE facilitation for different types of *coordinative* AOMI. Additionally, the single-pulse TMS technique adopted in this study only provides an indication of activity associated with *coordinative* AOMI within the motor and premotor cortices of the brain. Activity in other brain regions (e.g., rostral prefrontal cortex; Eaves, Behmer et al., 2016) would not have been represented in the MEP responses recorded in this experiment. There is a need to explore the precise anatomical substrates involved in different types of *coordinative* AOMI using neuroscientific methods with superior spatial resolution to TMS, such as functional magnetic resonance imaging (fMRI). FMRI research employing multi-voxel pattern analysis has shown it is possible to distinguish between different actions for MI and execution (Pilgramm et al., 2016; Zabicki et al., 2016). Applying this analysis to fMRI data for different types of *coordinative* AOMI could further advance the understanding of the neural mechanisms underpinning this form of dual-action simulation and provide more conclusive evidence regarding the propositions of the DASH (Eaves, Riach, et al., 2016) and VGH (Meers et al., 2020) accounts for *coordinative* AOMI.

732 In conclusion, the findings of this study lend possible support to both the DASH (Eaves, Riach, et
733 al., 2016) and VGH (Meers et al., 2020) propositions for *coordinative* AOMI. Specifically, in partial
734 support of the DASH, all three *coordinative* AOMI conditions resulted in increased CSE facilitation at the
735 stimulation timepoint aligned with the observed SL-STS, and at the respective stimulation timepoints
736 aligned with the imagined SL-STS movements. This aligned with propositions of the DASH that
737 sensorimotor representations for the observed and imagined SL-STS movements would merge during
738 $AOMI_{HICO}$ and $AOMI_{MOCO}$ due to the coordination between the simulated SL-STS movements, but this was
739 not expected for $AOMI_{LOCO}$ because of the increased competition between the observed and imagined
740 SL-STS movements. However, the current study offers more conclusive support for the VGH account of
741 *coordinative* AOMI as CSE was facilitated across all three stimulation timepoints, and CSE increased as
742 imagery speed increased across the *coordinative* AOMI conditions, indicating that imagery is likely
743 driving the CSE facilitation present in the data. However, the study design limits our ability to distinguish
744 between the contributions of AO and MI on a muscle-specific basis during *coordinative* AOMI. This study
745 provides novel neurophysiological evidence supporting for the use of *coordinative AOMI* as an
746 alternative method for (re)learning of movements that extend beyond a learner's repertoire, or for joint
747 actions that require coordination with the movements of others.
748
749

750 **References**

751 Ahmadi-Ahangar A, Shokri E, Khodadadi M, Ahangar R, Ahmadi-Ahangar A. 2018. The effect of
752 quadriceps muscle fatigue on postural control: a pilot study. *Chiropr Man Therap*. 26:19.
753 https://doi.org/10.1186/s12998-018-0195-x.

754 Alaerts K, de Beukelaar TT, Swinnen SP, Wenderoth N. 2012. Observing how others lift light or heavy
755 objects: time-dependent encoding of grip force in the primary motor cortex. Psychol Res. 76(4):503–
756 513. https://doi.org/10.1007/s00426-011-0380-1.

757 Alaerts K, Swinnen SP, Wenderoth N. 2010. Observing how others lift light or heavy objects: which visual
758 cues mediate the encoding of muscular force in the primary motor cortex? Neuropsychologia.
759 48(7):2082–2090. https://doi.org/10.1016/j.neuropsychologia.2010.03.029.

760 Alcazar J, Aagaard P, Haddock B, Kamper RS, Hansen SK, Prescott E, Alegre LM, Frandsen U, Suetta C.
761 2020. Age- and sex-specific changes in lower-limb muscle power throughout the lifespan. J Gerontol.
762 75(7):1369–1378. https://doi.org/10.1093/gerona/glaa013.

763 Bruton AM, Holmes PS, Eaves DL, Franklin ZC, Wright DJ. 2020. Neurophysiological markers discriminate
764 different forms of motor imagery during action observation. Cortex. 124:119–136.
765 https://doi.org/10.1016/j.cortex.2019.10.016.

766 Buccino G. 2014. Action observation treatment: a novel tool in neurorehabilitation. Philos Trans R Soc B.
767 369(1644):20130185. https://doi.org/10.1098/rstb.2013.0185.

768 Castro F, Bryjka PA, Di Pino G, Vuckovic A, Nowicky A, Bishop D. 2021. Sonification of combined action
769 observation and motor imagery: effects on corticospinal excitability. Brain Cogn. 152:105768.
770 https://doi.org/10.1016/j.bandc.2021.105768.

771 Castro F, Osman L, Di Pino G, Vuckovic A, Nowicky A, Bishop D. 2021. Does sonification of action
772 simulation training impact corticospinal excitability and audiomotor plasticity? Exp Brain Res.
773 239(5):1489–1505. https://doi.org/10.1007/s00221-021-06069-w.

774 Chen R, Gerloff C, Classen J, Wassermann EM, Hallett M, G Cohen L. 1997. Safety of different inter-train
775 intervals for repetitive transcranial magnetic stimulation and recommendations for safe ranges of
776 stimulation parameters. Electroencephalogr Clin Neurophysiol Electromyogr Mot Control.
777 105(6):415–421. https://doi.org/10.1016/s0924-980x(97)00036-2.
778 Chipchase L, Schabrun S, Cohen L, Hodges P, Ridding M, Rothwell J, Taylor J, Ziemann U. 2012. A
779 checklist for assessing the methodological quality of studies using transcranial magnetic stimulation
780 to study the motor system: an international consensus study. Clin Neurophysiol. 123(9):1698–1704.
781 https://doi.org/10.1016/j.clinph.2012.05.003.
782 Chye S, Valappil AC, Wright DJ, Frank C, Shearer DA, Tyler CJ, Diss CE, Mian OS, Tillin NA, Bruton AM.
783 2022. The effects of combined action observation and motor imagery on corticospinal excitability
784 and movement outcomes: two meta-analyses. Neurosci Amp Biobehav Rev. 143:104911.
785 https://doi.org/10.1016/j.neubiorev.2022.104911.
786 Cisek P. 2007. Cortical mechanisms of action selection: the affordance competition hypothesis. Philos
787 Trans R Soc B. [accessed 2024 Dec 4];362(1485):1585–1599.
788 https://doi.org/10.1098/rstb.2007.2054.
789 Clark S, Tremblay F, Ste-Marie D. 2004. Differential modulation of corticospinal excitability during
790 observation, mental imagery and imitation of hand actions. Neuropsychologia. 42(1):105–112.
791 https://doi.org/10.1016/s0028-3932(03)00144-1.
792 Condy EE, Miguel HO, Millerhagen J, Harrison D, Khaksari K, Fox N, Gandjbakhche A. 2021.
793 Characterizing the action-observation network through functional near-infrared spectroscopy: a
794 review. Front Hum Neurosci. 15. https://doi.org/10.3389/fnhum.2021.627983.
795 Cuypers K, Thijs H, Meesen RLJ. 2014. Optimization of the transcranial magnetic stimulation protocol by
796 defining a reliable estimate for corticospinal excitability. PLoS ONE. 9(1):e86380.
797 https://doi.org/10.1371/journal.pone.0086380.

798 Devanne H, Lavoie BA, Capaday C. 1997. Input-output properties and gain changes in the human
799 corticospinal pathway. Exp Brain Res. 114(2):329–338. https://doi.org/10.1007/pl00005641.
800 Eaves DL, Behmer LP, Vogt S. 2016. EEG and behavioural correlates of different forms of motor imagery
801 during action observation in rhythmical actions. Brain Cogn. 106:90–103.
802 https://doi.org/10.1016/j.bandc.2016.04.013.
803 Eaves DL, Hodges NJ, Buckingham G, Buccino G, Vogt S. 2022 Dec 27. Enhancing motor imagery practice
804 using synchronous action observation. Psychol Res. https://doi.org/10.1007/s00426-022-01768-7.
805 Eaves DL, Riach M, Holmes PS, Wright DJ. 2016. Motor imagery during action observation: a brief review
806 of evidence, theory and future research opportunities. Front Neurosci. 10.
807 https://doi.org/10.3389/fnins.2016.00514.
808 Filimon F, Rieth CA, Sereno MI, Cottrell GW. 2014. Observed, executed, and imagined action
809 representations can be decoded from ventral and dorsal areas. Cereb Cortex. 25(9):3144–3158.
810 https://doi.org/10.1093/cercor/bhu110.
811 Forster KI, Forster JC. 2003. DMDX: A Windows display program with millisec-sond accuracy. Behav Res
812 Methods Instrum Amp Comput. 35(1):116–124. https://doi.org/10.3758/bf03195503.
813 Grilc N, Valappil AC, Tillin NA, Mian OS, Wright DJ, Holmes PS, Castelli F, Bruton AM. 2024. Motor
814 imagery drives the effects of combined action observation and motor imagery on corticospinal
815 excitability for coordinative lower-limb actions. Sci Rep. 14(1). https://doi.org/10.1038/s41598-024-
816 63758-6.
817 Grosprêtre S, Ruffino C, Lebon F. 2015. Motor imagery and cortico-spinal excitability: a review. Eur J
818 Sport Sci. 16(3):317–324. https://doi.org/10.1080/17461391.2015.1024756.
819 Guillot A, Collet C. 2005. Duration of mentally simulated movement: a review. J Mot Behav. 37(1):10–
820 20. https://doi.org/10.3200/jmbr.37.1.10-20.

821 Hardwick RM, Caspers S, Eickhoff SB, Swinnen SP. 2018. Neural correlates of action: comparing meta-
822 analyses of imagery, observation, and execution. Neurosci Amp Biobehav Rev. 94:31–
823 44. https://doi.org/10.1016/j.neubiorev.2018.08.003.
824 Helm F, Marinovic W, Krüger B, Munzert J, Riek S. 2015. Corticospinal excitability during imagined and
825 observed dynamic force production tasks: effortfulness matters. Neuroscience. 290:398–
826 405. https://doi.org/10.1016/j.neuroscience.2015.01.050.
827 Hermens H, Freriks B, Merletti R, Stegeman D, Blok J, Rau G, Disselhorst-Klug C, Hagg G. 1999. European
828 recommendations for surface electromyography. Roessingh Research and Development.
829 Herranz-Gómez A, Gaudiosi C, Angulo-Díaz-Parreño S, Suso-Martí L, La Touche R, Cuenca-Martínez F.
830 2020. Effectiveness of motor imagery and action observation on functional variables: an umbrella
831 and mapping review with meta-meta-analysis. Neurosci Amp Biobehav Rev. 118:828–
832 845. https://doi.org/10.1016/j.neubiorev.2020.09.009.
833 Hess CW, Mills KR, Murray NM. 1987. Responses in small hand muscles from magnetic stimulation of the
834 human brain. J Physiol. 388(1):397–419. https://doi.org/10.1113/jphysiol.1987.sp016621.
835 Holmes P, Calmels C. 2008. A neuroscientific review of imagery and observation use in sport. J Mot
836 Behav. 40(5):433–445. https://doi.org/10.3200/jmbr.40.5.433-445.
837 Hughes MA, Myers BS, Schenkman ML. 1996. The role of strength in rising from a chair in the
838 functionally impaired elderly. *J Biomech*. 29:1509–1513. https://doi.org/10.1016/S0021-
839 9290(96)80001-7.
840 Jeannerod M. 2001. Neural simulation of action: a unifying mechanism for motor cognition.
841 NeuroImage. 14(1):S103–S109. https://doi.org/10.1006/nimg.2001.0832.
842 Kaneko N, Masugi Y, Yokoyama H, Nakazawa K. 2018. Difference in phase modulation of corticospinal
843 excitability during the observation of the action of walking, with and without motor imagery.
844 NeuroReport. 29(3):169–173. https://doi.org/10.1097/wnr.0000000000000941.

845 Kassambara A. 2023. R package version 0.7.2. Rstatix: pipe-friendly framework for basic statistical tests.
846 https://rpkgs.datanovia.com/rstatix/.
847 Keel JC, Smith MJ, Wassermann EM. 2001. A safety screening questionnaire for transcranial magnetic
848 stimulation. Clin Neurophysiol. 112(4):720. https://doi.org/10.1016/s1388-2457(00)00518-6.
849 Kitamura M, Yamamoto K, Oshima A, Kamibayashi K. 2023. Corticospinal excitability during observation
850 of basketball free-throw movement: effects of video playback speed and stimulus timing. Plos One.
851 18(9):e0292060. https://doi.org/10.1371/journal.pone.0292060.
852 Loporto M, Holmes PS, Wright DJ, McAllister CJ. 2013. Reflecting on mirror mechanisms: motor
853 resonance effects during action observation only present with low-intensity transcranial magnetic
854 stimulation. PLoS ONE. 8(5):e64911. https://doi.org/10.1371/journal.pone.0064911.
855 Loporto M, McAllister CJ, Edwards MG, Wright DJ, Holmes PS. 2012. Prior action execution has no effect
856 on corticospinal facilitation during action observation. Behav Brain Res. 231(1):124–129.
857 https://doi.org/10.1016/j.bbr.2012.03.009.
858 Lord SR, Murray SM, Chapman K, Munro B, Tiedemann A. 2002. Sit-to-stand performance depends on
859 sensation, speed, balance, and psychological status in addition to strength in older people. *J*
860 *Gerontol A Biol Sci Med Sci*. 57:M539–M543. https://doi.org/10.1093/gerona/57.8.M539.
861 MacIntyre TE, Moran AP, Collet C, Guillot A. 2013. An emerging paradigm: a strength-based approach to
862 exploring mental imagery. Front Hum Neurosci. 7. https://doi.org/10.3389/fnhum.2013.00104.
863 Marusic U, Grosprêtre S, Paravlic A, Kovač S, Pišot R, Taube W. 2018. Motor imagery during action
864 observation of locomotor tasks improves rehabilitation outcome in older adults after total hip
865 arthroplasty. Neural Plast. 2018:1–9. https://doi.org/10.1155/2018/5651391.
866 McCormick SA, Ireland C, Yohannes AM, Holmes PS. 2022. Technology-Dependent rehabilitation
867 involving action observation and movement imagery for adults with stroke: can it work? Feasibility

868 of self-led therapy for upper limb rehabilitation after stroke. Stroke Res Treat. 2022:1–10.
869 https://doi.org/10.1155/2022/8185893.
870 Meers R, Nuttall HE, Vogt S. 2020. Motor imagery alone drives corticospinal excitability during
871 concurrent action observation and motor imagery. Cortex. 126:322–333.
872 https://doi.org/10.1016/j.cortex.2020.01.012.
873 Miyoshi K, Kimura T, Yokokawa Y, Cheng GA, Fujiwara T, Yamamoto I, Kondo Y. 2005. Effect of ageing on
874 quadriceps muscle strength and on the forward shift of center of pressure during sit-to-stand
875 movement from a chair. *J Phys Ther Sci*. 17(1):23–28. https://doi.org/10.1589/jpts.17.23.
876 Mizuguchi N, Umehara I, Nakata H, Kanosue K. 2013. Modulation of corticospinal excitability dependent
877 upon imagined force level. Exp Brain Res. 230(2):243–249. https://doi.org/10.1007/s00221-013-
878 3649-3.
879 Moreno-Verdú M, Hamoline G, Van Caenegem EE, Waltzing BM, Forest S, Chembila Valappil A, Khan AH,
880 Chye S, Esselaar M, Campbell MJ, et al. 2023 Nov. Guidelines for reporting action simulation studies
881 (GRASS): proposals to improve reporting of research in motor imagery and action observation.
882 Neuropsychologia. 108733. https://doi.org/10.1016/j.neuropsychologia.2023.108733.
883 Moriuchi T, Iso N, Sagari A, Ogahara K, Kitajima E, Tanaka K, Tabira T, Higashi T. 2014. Excitability of the
884 primary motor cortex increases more strongly with slow- than with normal-speed presentation of
885 actions. PLoS ONE. 9(12):e114355. https://doi.org/10.1371/journal.pone.0114355.
886 Moriuchi T, Matsuda D, Nakamura J, Matsuo T, Nakashima A, Nishi K, Fujiwara K, Iso N, Nakane H,
887 Higashi T. 2017. Primary motor cortex activation during action observation of tasks at different video
888 speeds is dependent on movement task and muscle properties. Front Hum Neurosci. 11.
889 https://doi.org/10.3389/fnhum.2017.00010.

890 Mouthon A, Ruffieux J, Wälchli M, Keller M, Taube W. 2015. Task-dependent changes of corticospinal
891 excitability during observation and motor imagery of balance tasks. Neuroscience. 303:535–543.
892 https://doi.org/10.1016/j.neuroscience.2015.07.031.
893 Mouthon AA, Ruffieux J, Keller M, Taube W. 2016. Age-Related differences in corticospinal excitability
894 during observation and motor imagery of balance tasks. Front Aging Neurosci. 8.
895 https://doi.org/10.3389/fnagi.2016.00317.
896 Naish KR, Houston-Price C, Bremner AJ, Holmes NP. 2014. Effects of action observation on corticospinal
897 excitability: muscle specificity, direction, and timing of the mirror response. Neuropsychologia.
898 64:331–348. https://doi.org/10.1016/j.neuropsychologia.2014.09.034.
899 Nicholson V, Watts N, Chani Y, Keogh JW. 2019. Motor imagery training improves balance and mobility
900 outcomes in older adults: a systematic review. J Physiother. 65(4):200–207.
901 https://doi.org/10.1016/j.jphys.2019.08.007.
902 Pilgramm S, de Haas B, Helm F, Zentgraf K, Stark R, Munzert J, Krüger B. 2015. Motor imagery of hand
903 actions: decoding the content of motor imagery from brain activity in frontal and parietal motor
904 areas. Hum Brain Mapp. 37(1):81–93. https://doi.org/10.1002/hbm.23015.
905 Riach M, Wright DJ, Franklin ZC, Holmes PS. 2018. Screen position preference offers a new direction for
906 action observation research: preliminary findings using TMS. Front Hum Neurosci. 12.
907 https://doi.org/10.3389/fnhum.2018.00026.
908 Roberts R, Callow N, Hardy L, Markland D, Bringer J. 2008. Movement imagery ability: development and
909 assessment of a revised version of the vividness of movement imagery questionnaire. J Sport Exerc
910 Psychol. 30(2):200–221. https://doi.org/10.1123/jsep.30.2.200.
911 Robinovitch SN, Feldman F, Yang Y, Schonnop R, Leung PM, Sarraf T, Loughin M. 2013. Video capture of
912 the circumstances of falls in elderly people residing in long-term care: an observational study.
913 *Lancet*. 381(9860):47–54. https://doi.org/10.1016/S0140-6736(12)61263-X

914 Rossini PM, Burke D, Chen R, Cohen LG, Daskalakis Z, Di Iorio R, Di Lazzaro V, Ferreri F, Fitzgerald PB,
915 George MS, et al. 2015. Non-invasive electrical and magnetic stimulation of the brain, spinal cord,
916 roots and peripheral nerves: basic principles and procedures for routine clinical and research
917 application. an updated report from an I.F.C.N. committee. Clin Neurophysiol. 126(6):1071–1107.
918 https://doi.org/10.1016/j.clinph.2015.02.001.
919 Rothwell JC. 1997. Techniques and mechanisms of action of transcranial stimulation of the human motor
920 cortex. J Neurosci Methods. 74(2):113–122. https://doi.org/10.1016/s0165-0270(97)02242-5.
921 Schenkman M, Hughes MA, Samsa G, Studenski S. 1996. The relative importance of strength and balance
922 in chair rise by functionally impaired older individuals. *J Am Geriatr Soc*. 44:1441–1446.
923 Scott M, Taylor S, Chesterton P, Vogt S, Eaves DL. 2018. Motor imagery during action observation
924 increases eccentric hamstring force: an acute non-physical intervention. Disabil Rehabil.
925 40(12):1443–1451. https://doi.org/10.1080/09638288.2017.1300333.
926 Slaughter SE, Wagg AS, Jones CA, Hemmelgarn BR, Sadowski CA. 2015. Mobility of Vulnerable Elders
927 Study: Effect of the sit-to-stand activity on mobility, function, and quality of life. *J Am Med Dir*
928 *Assoc*. 16(2):138–143. https://doi.org/10.1016/j.jamda.2014.08.015.
929 Tapanya W, Chamnongkich S. 2014. Relationship between lower limb muscle strength and single-leg sit-
930 to-stand performance in young adults. *Bull Chiang Mai Assoc Med Sci*. 47(3):133. https://he01.tci-
931 thaijo.org/index.php/bulletinAMS/article/view/59978
932 Tatemoto T, Tsuchiya J, Numata A, Osawa R, Yamaguchi T, Tanabe S, Kondo K, Otaka Y, Sugawara K.
933 2017. Real-time changes in corticospinal excitability related to motor imagery of a force control task.
934 Behav Brain Res. 335:185–190. https://doi.org/10.1016/j.bbr.2017.08.020.
935 Taube W, Lorch M, Zeiter S, Keller M. 2014. Non-physical practice improves task performance in an
936 unstable, perturbed environment: motor imagery and observational balance training. Front Hum
937 Neurosci. 8. https://doi.org/10.3389/fnhum.2014.00972.

938 Thongchoomsin S, Bovonsunthonchai S, Joseph L, Chamnongkich S. 2020. Clinimetric properties of the
939 one-leg sit-to-stand test in examining unilateral lower limb muscle strength among young adults.
940 *Int J Clin Pract*. 74:e13480. https://doi.org/10.1111/ijcp.13480.
941 Tremblay, Louis E Tremblay, Daniel F. 2001. Modulation of corticospinal excitability during imagined
942 knee movements. J Rehabil Med. 33(5):230–234. https://doi.org/10.1080/165019701750419635.
943 Vogt S, Rienzo FD, Collet C, Collins A, Guillot A. 2013. Multiple roles of motor imagery during action
944 observation. Front Hum Neurosci. 7. https://doi.org/10.3389/fnhum.2013.00807.
945 Wickham H (2016). ggplot2: Elegant Graphics for Data Analysis. Springer-Verlag New York. ISBN 978-3-
946 319-24277-4, https://ggplot2.tidyverse.org.
947 Williams J, Pearce AJ, Loporto M, Morris T, Holmes PS. 2012. The relationship between corticospinal
948 excitability during motor imagery and motor imagery ability. Behav Brain Res. 226(2):369–375.
949 https://doi.org/10.1016/j.bbr.2011.09.014.
950 Wright DJ, Williams J, Holmes PS. 2014. Combined action observation and imagery facilitates
951 corticospinal excitability. Front Hum Neurosci. 8. https://doi.org/10.3389/fnhum.2014.00951.
952 Wright DJ, Wood G, Eaves DL, Bruton AM, Frank C, Franklin ZC. 2018. Corticospinal excitability is
953 facilitated by combined action observation and motor imagery of a basketball free throw. Psychol
954 Sport Exerc. 39:114–121. https://doi.org/10.1016/j.psychsport.2018.08.006.
955 Wright DJ, Frank C, Bruton AM. 2022. Recommendations for combining action observation and motor
956 imagery interventions in sport. J Sport Psychol Action. [accessed 2024 Dec 6]:1–
957 13. https://doi.org/10.1080/21520704.2021.1971810.
958 Zabicki A, de Haas B, Zentgraf K, Stark R, Munzert J, Krüger B. 2016 Sep 6. Imagined and executed
959 actions in the human motor system: testing neural similarity between execution and imagery of
960 actions with a multivariate approach. Cereb Cortex. https://doi.org/10.1093/cercor/bhw257.